Kinetic and Isotherm Studies of Methyl Violet Adsorption onto Carbonized Waterlily (Nymphaea lotus) Leaves Powder

Abdullahi Muhammad Ayuba [1], Hamisu Abdulmumini [2], Mohammed Mukhtar Mohammed [2], Solomon Daniel [2]

[1] *Bayero University Kano*
Nigeria Gwarzo Road, P. M. B. 3011, Kano, Nigeria

[2] *Abubakar Tatari Ali Polytechnic*
P. M. B. 0094, Bauchi, 740272, Nigeria

DOI: 10.22178/pos.90-16

LCC Subject Category: L7-991

Received 09.02.2023
Accepted 28.03.2023
Published online 31.03.2023

Corresponding Author:
Hamisu Abdulmumini
hamisulame41@gmail.com

Abstract. In this study, the adsorption of methyl violet from an aqueous solution using carbonised water lily (CWL) leaves powder as a low-cost, efficient and eco-friendly adsorbent was investigated using a batch system under controlled conditions. The adsorbent's moisture, organic matter, ash, bulk density, pore volume, and pH were determined. The adsorbents were characterised by scanning electron microscopy (SEM) and Fourier Transform Infrared (FT-IR) techniques which confirm the adsorption of the methyl violet onto the CWL adsorbents. The effect of adsorption parameters such as contact time, dosage, initial concentration, pH and temperature were studied for optimisation. It was confirmed that contact time, dosage, concentration, pH and temperature positively affected adsorption. The kinetic data were best described by pseudo-second order under all experimental temperatures. The adsorption isotherms were estimated and established to fit nicely into the D-R model compared to other models generated and tested. Thermodynamic studies of the sorption process indicate that the process was feasible, spontaneous, and exothermic and decrease in the randomness of the adsorption process during the transfer of molecules between the adsorbent and adsorbates with entropy (ΔS) of 23.77 J/mol.K. due to negative values of Gibb's free energy observed. This study confirmed that CWL could be employed as a low-cost, eco-friendly adsorbent for removing toxic dyes such as methyl violet from an aqueous solution.

Keywords: carbonised water lily; equilibrium; thermodynamics; adsorption; kinetics; isotherms.

INTRODUCTION

Various techniques and methods have been developed and widely employed to combat excessive colourant water discharges (wastewater) from textiles, leather, paper, pulps, petrochemicals, pharmaceuticals, and food and beverages industries [1]. These wastewater contaminants pose a significant environmental threat, threatening the ecosystem [2]. According to [3], the treatment of dye wastewater is not only an essential but also a challenging task faced by many countries worldwide, particularly industrialised ones. As such, getting rid of these contaminants before releasing them into the environment is essential. Due to financial considerations, Conventional wastewater treatment methods such as coagulation, ultra-filtration, ozonation, oxidation, sedimentation, reverse osmosis, floatation, and precipitation are highly challenging [4]. As a result, the adsorption method approach has been used in recent years over conventional methods due to its efficiency, low operating cost, procedure flexibility and simplicity of operation in removing pollutants from effluents to stable forms [5].

Beautiful aquatic flowering plants known as water lilies are widely used decorative plants, cultural icons and commercial commodities. This plant is found in the underwater section of nearly every botanic garden because of its highly prized

ornamental characteristics. The entire spectrum of petal colours ranges from black to white, making it the most diversely coloured flowering plant, as shown in Figure 1 [6]. Beyond being beautiful ornamental plants, this plant has been utilised as an ingredient in numerous goods, including cosmetics, soap, perfume, hand lotion, floral tea bags, and traditional medicines [7]. Despite this noble plant's purported use, there is limited published information about using it as an adsorbent.

According to the literature, several biomasses have been employed to remove different forms of methyl violet from aqueous solution successfully. Acid-modified activated carbon [1]; activated carbon derived from coffee residues [8]; magnetic composite [9]; copper pod flower [10]; chromium phopovanadate (Cr-PV) nanoparticles [11]; rice husk powder [12], activated carbon Oak wood [13], Hagenia abyssinica leaf powder [14], Parkia speciosa hassk peel [15]. This research did not discover the utilisation of carbonised water lily leaves as an adsorbent for removing methyl violet from an aqueous solution. It's important to note that [16] evaluated the adsorptive potential of different water lily parts such as leaves, shoots and roots. Still, their research was limited to removing heavy metals such as Cd and Pb from aqueous solutions.

So, this work aims to investigate the potential of carbonised water lily (CWL) leaves as inexpensive adsorbents for removing methyl violet from aqueous solutions under optimal contact time, dose, initial concentration, pH, and temperature conditions, respectively. Isotherms, kinetic models, thermodynamic parameters, and surface characterisations were investigated and reported accordingly.

MATERIALS AND METHODS

Chemical, Reagents and Apparatus. All the chemicals, reagents and materials used in this research were of analytical grade and collected and used without further purification. These include potassium hydroxide (KOH), sodium hydroxide (NaOH), hydrochloric acid (HCl), pestle and mortar, beakers, conical flask, volumetric flask, sieve, distilled water, filter paper (whatman No 1), funnels, glass rod while Methyl violet (MV) dye.

Sample Collection & Adsorbent Preparation. The water lily leaves (WLL) were obtained from Gubi Dam, Bauchi State. The leaves were washed thoroughly with distilled water and shade dried for 72 hours. The carbonised adsorbents (CWL) were prepared in a muffle furnace. Leaves were ground and segregated to granular mesh size with an earlier semi-carbonisation for 15 min at an initial temperature of 200 °C. The furnace temperature was adjusted to a desired temperature of 500 °C for 45 min for the sample to undergo complete carbonisation [17]. The piece was dried, ground and sieved to obtain a working size of 300 μm and finally, the powder was stored in an air-tight container for further experimental studies.

Determination of Ash & Moisture Content. The ash and moisture contents were determined by weight difference [16]. For moisture content, 1 g of the ground leaves were heated at 80 °C for 3 hours. Cooled in a desiccator and weighed. The procedure was repeated several times at the same temperature for 15 min until constant weights were obtained. The percentage moisture content of the sample was determined using (1).

$$\% \text{ Moisture content} = \frac{W1-W3}{W2-W1}\text{x}100 \quad (1)$$

where w1 is the weight of the empty crucible, w2 is the weight of the crucible and the sample after heating, and w3 is the final weight of the crucible and the model after heating.

In determining Ash content, 1 g was placed in a crucible of known weight and then heated at 500 °C for 3 hours. The sample was cooled in a desiccator and weighed. The ash content of each sample was calculated from the weight of the sample before and after heating as (2):

$$\% \text{ Ash content} = \frac{W1-W3}{W2-W1}\text{x}100 \quad (2)$$

where w1 is the initial weight of the crucible, w2 is the initial weight of the crucible and the sample before heating, and w3 is the final weight of the piece and the crucible.

Determination of Organic Matter Content. The organic matter contents of the adsorbents were determined from the difference between the 100% air-dried adsorbent measured and the percentage ash content [18] as illustrated in the (3):

% Organic matter content=

$$= 100 - \%Ash\ content \quad (3)$$

Determination of pH. 1 g of the sample was put inside a 250 ml Erlenmeyer flask. Then 100 ml of distilled water was poured into the flask. The solution was heated for 15 minutes in a boiling condition. The answer was cooled at room temperature and diluted with distilled water to 100 ml. The answer was stirred well, and the pH was determined using a pH meter [19].

Pore (Void) Volume Determination. To determine the pore volume of the adsorbents, the method reported by [20] was adopted. 2.0 g of the samples (RWL, CWL and AWL) was immersed in water and boiled for 15 min. After the air in the pores had been displaced, the piece was dried superficially and reweighted. The increase or difference in weight is divided by the water given the pore volume.

$$\text{Pore (void)volume} = \frac{W2-W1}{density\ of\ water} \quad (4)$$

where w1 is the weight of an empty density bottle, w2 is the weight of the density bottle and sample together and the density of water is 1 g/cm^3.

Bulk Density (Apparent Density) Determination. The bulk density of the sample was determined to know the packed density of a piece. It's carried out according to the procedure reported by [21].

$$Bulk\ density = \frac{\left(weight\ of\ the\ sample\left(\frac{g}{ml}\right)\right)}{100} \quad (5)$$

Preparation of Stock Solution. A stock solution of Malachite green and methyl violet dyes (Figure 1) was prepared by dissolving 1 g of each shade in a 1000 ml volumetric flask at room temperature and shaking until a homogenous solution was obtained [18].

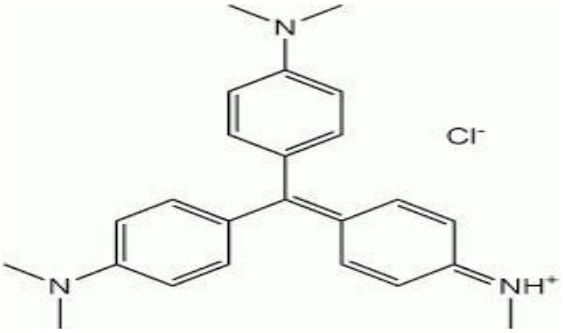

Figure 1 – Structure of methyl violet dye

The sample of the required concentration was prepared by diluting the stock solution with distilled water to the required concentration using the (6):

$$C_1V_1 = C_2V_2 \quad (6)$$

Optimisation of Experimental Parameters. The effect of contact time on the adsorption of the dyes used in these experiments was conducted at room temperature. An initial concentration of the adsorbates of 100 mg/l, adsorbents dose of 0.1 g for raw, modified and carbonised adsorbent was introduced and shaken at 150 rpm [22]. The data generated from this study at 5-120 minutes respectively was used for adsorption kinetics studies.

Method [23] was adopted with minor adjustments. The effect of adsorbent dosage was studied and carried out with an initial concentration of 100 mg/l at different dosage amounts of 0.02, 0.05, 0.08, 0.1 and 0.2 g, respectively. The weighed samples were taken in polythene bottles with 50 ml of the stock solution. The model was kept in an orbital shaker at room temperature, constant speed of 150 rpm at the optimum time.

Concentration is among the critical factors influencing the rate of chemical reactions. The effect of the variation in the initial concentration of dye solution at room temperature using a fixed amount of the adsorbents was determined by using 30, 60, 90, 120, 150 and 180 ppm initial concentration of methyl violet dye. The mixture was then shaken at the optimum time, room temperature and adsorbent dosage of 0.02 g at a speed of 150 rpm. The solution was filtered using whatman filter paper, and the filters were then taken for UV-spectrophotometric analysis.

The adsorption experiment was carried out at different pH to determine the optimum pH for the adsorption process. The optimum initial concentration and adsorbent dosage were added into five other polythene bottles (50 ml), with each bottle conditioned at different pH (3, 5, 7, 9, 11 and 13) and room temperature, respectively. The pH was adjusted to a desired value with 0.1 M HCl or 0.1 M NaOH solution. The bottles were shaken at 150 rpm, and they were then filtered. The filter was analysed using UV-spectrophotometer to determine the concentration of residual (un-adsorbed) dyes [24, 25].

Adsorption Equilibrium Experiments. Batch adsorption was adopted for this experiment because of its simplicity [26]. The batch experiments were carried out to determine the optimum conditions for equilibrium adsorption of MV dye onto CWL adsorbent. The results obtained after optimisation experiments were used to conduct the batch adsorption for the six different systems at their ideal conditions. These systems were run separately in 60 cm^3 polyethene sample bottles at 30, 40, 50 and 60 °C temperatures. The samples were placed in a temperature-controlled shaker for the period reported for each system. After reaching the equilibrium period, the content was filtered, and the filtrate was analysed using Perkin-Elemer UV-visible Spectrophotometer at a maximum absorbance wavelength of 582.37 nm of MV dye. The amount of the adsorbed dye was obtained using (7):

$$Qe = \frac{(C0-Ce)}{M} x\ V \quad (7)$$

While colour removal rate (%Removal) was calculated using (8):

$$\%R = \frac{(Co-Ce)}{Co}\ x\ 100 \quad (8)$$

where q_e is adsorption capacity (mg/g), C_o and C_e are the initial and final concentration in (mg/l) respectively for the dyes in the solution, V is the volume of the dyes in solution (L), and m is the mass of the adsorbents [18, 26].

FTIR Analysis. Fourier transform infrared spectroscopy was used to study the adsorbents' surface functional group so that the prepared adsorbents' chemical structure is then determined. IR spectra were obtained with a type spectrum 100 series FTIR spectrometer (Agilent Technology Perkin Elmer Spectrum 100, USA) using the transformation of 20 scans with a spectral resolution of 4 cm^{-1} by attenuated total reflectance method. FTIR spectra were collected in the mid-infrared region between 4,000 and 650 cm^{-1}. Air background correction acquired Spectra [17].

Scanning Electron Microscope Analysis. Scanning electron microscope (SEM) is an analysis of the surface morphology of the adsorbents and was carried out by viewing the electron micrographs of the materials [27]. The research was done with a proxy Scanning Electron Microscope (phenom world Eindhoven). A thin layer of adhesive, carbon glue, was attached to a stub in sample preparation for the SEM analysis. A minimal amount of the materials to be viewed was spread on the stub materials and subsequently viewed in the instrument to obtain micrographs. Scanned micrographs of CWL before and after adsorption were taken at an accelerating voltage of 15.00 kv and 1500 X magnification.

RESULTS AND DISCUSSION

Physicochemical properties of the adsorbents. Table 1 shows the physical properties of the adsorbents prepared.

Table 1 – Physicochemical properties of the prepared adsorbents

Parameters	Values
Moisture contents (%)	12.30±0.43
Ash contents (%)	20.04±0.21
Organic matter (%)	79.96±0.20
pH	8.97±0.20
Pore volume (cm3)	1.98±0.01
Bulk density (g/dm3)	0.209±0.07

The moisture content value of 12.30% was recorded, significantly lower than the 53.41% reported for cassava stem biochar [28]. Still, the ash content value was 20.04%, indicating many inorganic substances that could be recovered after completely combusting the sample's biomass. This result is lower than the values obtained for water lettuce leaves (23.20%). Water lily stems (22.00%) and higher than the values reported for rice husk briquette (16.10%), melon shell (19.57%) and water hyacinth stem (19.80%) [29,

30]. Organic matter refers to the part of the sample's biomass that releases when heated (400-900 °C). The biomass decomposes into volatile gas and solid char during the heating process. The sample's biomass has high flammable matter contents of 79.96%. This value is higher than the volatile content of 67.08% and 57.23% for water hyacinth and lettuce leaves reported [29].

The pH of the samples was found to be 8.97, which is slightly above the 6-8 range for acceptable pH for applications of adsorbents, as reported by [31]. The bulk density recorded for this research was 0.209 g/dm^3. This parameter is an essential physical factor, especially when an activated carbon product is to be investigated for its filterability. This is because it determines the mass of carbon that can be contained in the filter of a given solid capacity and the amount of treated liquid that can be retained by filter paper [32].

Characterisation of the Adsorbents. Figure 2 shows the FT-IR spectra of the adsorbents before and after the adsorption of methyl violet dyes. The FT-IR spectra demonstrate or indicate the presence of functional groups on the surface of CWL before and after the adsorption of methyl violet dye molecules.

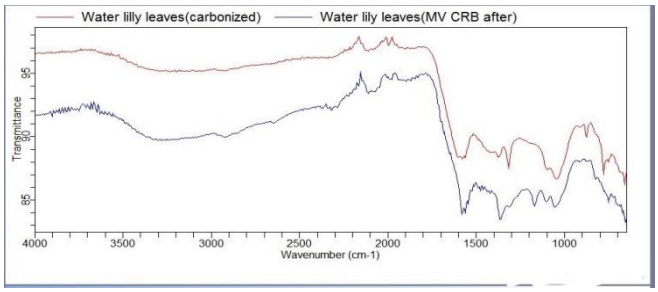

Figure 2 – The FT-IR spectra of CWL adsorbents before and after adsorption of MV dyes

Before adsorption, absorption bands at

3438 cm^{-1}, 2951 cm^{-1}, 1623 cm^{-1}, 1385 cm^{-1} and 1097 cm^{-1} were attributed to hydroxyl groups, aliphatic C-H group, carboxylic groups, C-O stretch and C-H aromatic ring vibration peaks respectively. After adsorption, there was a shift and broadening of the absorption peaks. Notably, the aromatic carbon-carbon double bond was observed at 1582 cm^{-1}, absent before adsorption. The changes of O-H, C-H, carboxylic groups, C=C and C-H aromatic rings peaks indicate the involvement of these functional groups in the adsorption of methyl violet dye molecules. Therefore, the changes in FT-IR spectra confirmed that carbonised water lily leaves (CWL) adsorbents could be helpful to adsorbents for removing dyes and heavy metals. The same observation was reported [33, 34].

To investigate the surface morphology of CWL, SEM analysis was conducted. Figures 3a and 3b show the surface of the biosorbent both before and after the adsorption of MV dye. The SEM micrograph in Figure 3a shows a rough surface with irregular cracks that may aid adsorption. After the adsorption of MV onto CWL, as presented in Figure 3b, the surface smoothens, and the pores are filled with the deposit of MV dye molecules onto the CWL adsorbents surface. These pores provided a good feeling for dyes, heavy metals and waste effluents to be trapped and adsorbed into [35, 36].

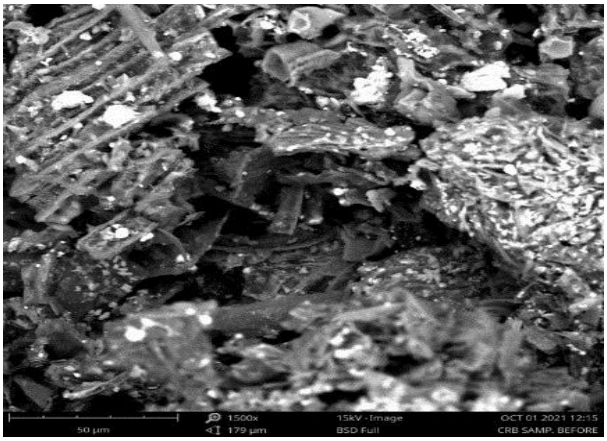

a)

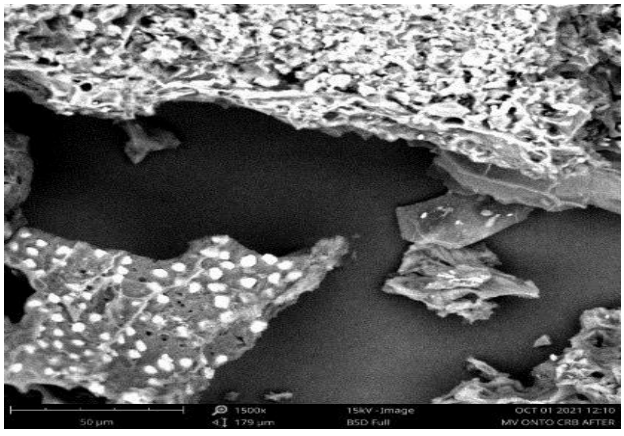

b)

Figure 3 – SEM micrograph of CWL adsorbents (a) before adsorption of methyl violet, (b) after adsorption of methyl violet dye

Optimisation Studies

Figure 4a demonstrates the steady rise in adsorption for the first 90 mins.

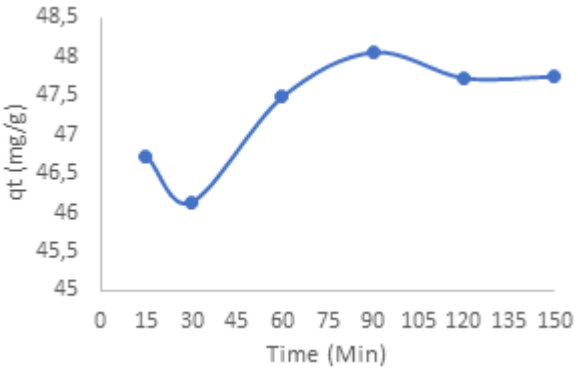

Figure 4a – Effect of Contact Time, (b) Dosage on adsorption of MV onto CWL adsorbent

This continued rise in the sorption rate recorded at the initial period of the process could be partly associated with the availability of many vacant sites on the adsorbent surface that are available for the rapid adsorption and accommodation of the MV molecules. After a time lapse (90 min), the large vacant sites of RWL that were available at the beginning of the adsorption of MV from the solution had become inaccessible or exhausted [21]. Subsequently, increasing the agitation time beyond 90 mins decreases the adsorption of the methyl violet dyes. These could be attributed to the desorption of the dye molecules on the available adsorption sites on the adsorbent materials as equilibrium conditions are established [37, 38].

Figure 4b shows a plot for the variation of adsorbent dosage with the amount of methyl violet dye adsorbed.

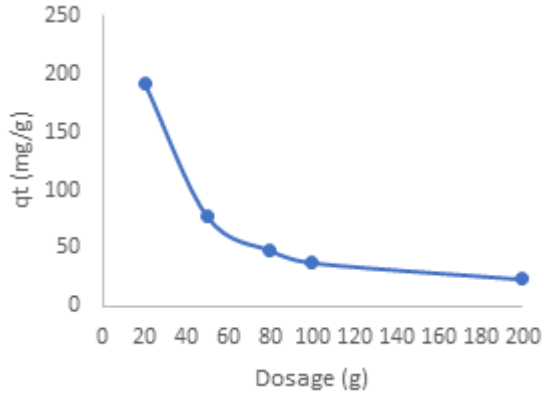

Figure 4b – Effect of Dosage on adsorption of MV onto CWL adsorbent

The results show that increasing the adsorbent dosage decreases the adsorption capacity of adsorbents. There are two factors which contribute to the adsorbent mass effect: 1) as the dosage increases, the adsorption sites remain unsaturated during the adsorption reaction leading to a drop in adsorption capacity [39]; 2) the aggregation/agglomeration of the adsorbent particles at higher mass could lead to a decrease in the surface area and increase in diffusional path length [40].

Figure 5a shows a plot of the variation of the amount of MV adsorbed concerning the initial concentration of methyl violet. From the field, the amount of MV adsorbed by CWL increases with increasing concentration. At lower concentrations, the available driving force for the transfer of MV molecules onto CWL is standard. In comparison, at higher concentrations, there was an increase in driving force, which enhanced the interaction between the MV molecules in the aqueous phase and the vacant active sites of the CWL adsorbents, hence the increase in the MV uptake [41].

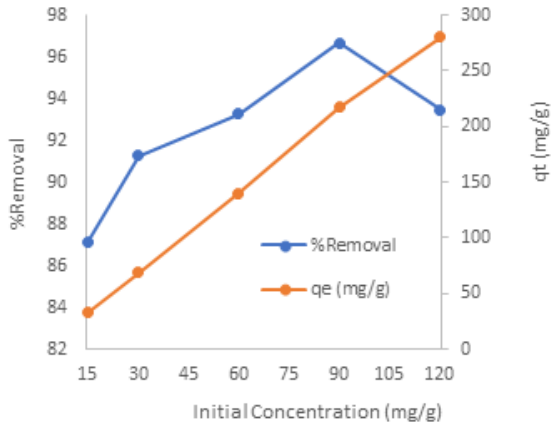

a)

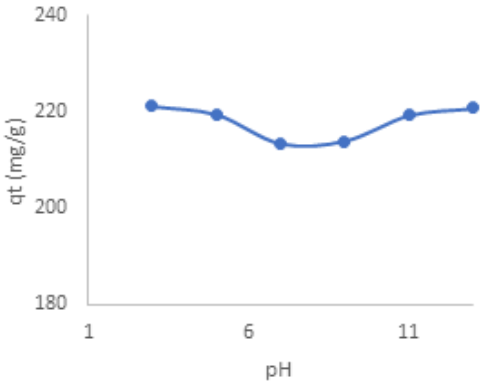

b)

Figure 5 – Effect of a) Initial Concentration, b) pH on adsorption of MV onto CWL adsorbents

The percent removal increases gradually at lower concentrations until it reaches a maximum before rapidly decreasing. This is because the vacant or active sites on the CWL surface become saturated or inaccessible by CWL adsorbents.

The effect of pH was studied by varying the pH from 3–13 while keeping other operating parameters constant. A plot of the variation in the amount of MV adsorbed is shown in Figure 5b. The amount of MV adsorbed by CWL increases significantly as the pH of the solution is adjusted from acidic to basic. This case is usual, as most studies show that an increase in the removal of adsorbates is observed with increasing pH [42, 43].

The Kinetic studies

The study of kinetic models could provide helpful information about the mechanism and the efficiency of the adsorption process [44]. For this study, the adsorption time was varied from 5 to 60 mins with intervals of 5 mins, where other operating parameters were kept at optimised conditions at temperatures of 30, 40 and 50 °C, respectively. Pseudo-first order, pseudo-second order, elvish and intraparticle diffusion models were employed to analyse kinetic data generated for MV adsorption onto CWL adsorbents.

Pseudo-first-order kinetic model. The pseudo-first-order equation is usually expressed according to (9):

$$\frac{dq_t}{dt} = k_1(q_e - q_t) \quad (9)$$

where qe and qt are the amount adsorbed per unit mass of the adsorbent at equilibrium and time t respectively (mg/g), k_1 is the rate constant of pseudo first order sorption rate (min 1), given a boundary condition for t=0 and $q_t = 0$ [45].

Equation (9) can be integrated into (10):

$$\log(q_e - q_t) = \log q_e - \frac{k_1 t}{2.303} \quad (10)$$

The plot of $\log(q_e\text{-}q_t)$ vs t gives a linear relationship from which k_1 and qt were determined from the slope and the intercept of $\log(q_e\text{-}q_t)$ against t.

The plot of $\log(q_e\text{-}q_t)$ vs t should give a linear relationship, from which k_1 and qe were determined from the slope and intercept of the story presented in Table 2. The R^2 values calculated were not close to unity, and Q_{cal} was lower than the experimental Q_{exp} one at all experiment temperatures, indicating that the pseudo-first-order model did not fit to describe the kinetic data generated.

Pseudo-second-order kinetic model. The pseudo-second-order adsorption kinetic model is expressed in (11).

$$\frac{dq_t}{dt} = k_1(q_e - q_t)^2 \quad (11)$$

where k_2 is the rate constant for the pseudo-second-order model (mg/min), applying the boundary conditions t =0 to t=t and q_t=0 to q_t=q_t.

The integral form of (11) becomes:

$$\frac{t}{q_t} = \frac{1}{k_2 q_e^2} + \frac{1}{q_e} \quad (12)$$

where k_2 is the rate constant of adsorption (mg/min), q_e and q_t are the amounts of dye adsorbed at equilibrium and at time t (mg/g), respectively.

The plot of t/q_t vs t gives a linear relationship for which qe and k_2 were determined from the slope and intercept of t/q_t against t, respectively.

The k_2 and Q_{cal} were obtained from the intercepts ($1/k_2q_e^2$) and the slope ($1/q_e$) of the plots t/q_e vs t and presented in Table 2.

The correlation coefficient of pseudo-second order was close to unity. Q_{cal} values computed from pseudo-second-order equations showed good agreement with experimental data, indicating the applicability of pseudo-second-order kinetic models for the CWL-MV system at all the temperatures of the experiments. Therefore, this model fits the kinetic data of the systems generated.

Table 2 – Kinetic model parameters for the adsorption of MV onto CWL adsorbents.

Kinetic Model	Parameters				
Pseudo-first order		Q_{exp} (mg/g)	Q_{cal} (mg/g)	k_1 (min^{-1})	R^2
	30 °C	221.21	0.722	$-3.82x10^{-2}$	0.3263
	40 °C	218.62	1.350	$-389x10^{-2}$	0.4165
	50 °C	208.95	4.980	$5.64x10^{-2}$	0.1412
Pseudo-first order		Q_{exp} (mg/g)	Q_{cal} (mg/g)	k_2 (mg/gmin)	R^2
	30 °C	221.21	217.39	$-3.02x10^{-3}$	0.9990
	40 °C	218.62	208.33	$-9.60x10^{-3}$	0.9985
	50 °C	208.95	196.08	$-7.22x10^{-2}$	0.9929
Elovich model			β	α	R^2
	30 °C		-.05360	-1.854	0.1420
	40 °C		-0.222	-4.416	0.4343
	50 °C		-0.426	-2.321	0.1864
Intraparticle diffusion			C	Kint	R2
	30 °C		221.58	-0.778	0.1310
	40 °C		222.52	-1.934	0.4343
	50 °C		205.73	-1.011	0.077

The Elovich Model. The Elovich kinetic model is described by (13).

$$q_t = \frac{1}{\beta}\ln(\alpha\beta) + \frac{1}{\beta} lnt \quad (13)$$

The parameters αβ are the initial rate constant (mg/min) and desorption constant and were calculated from the slope and intercept of the plot of q_t vs ln(t). This model gives valuable information and explanation on the extent of both surface activity and activation energy for the adsorption process [46].

The R^2 values obtained for this model were all≤0.4343 at all experimental temperatures, which is not close to unity. These deviations from linearity (R^2 not closed to agreement) reflect or suggest that this model does not fit the kinetic data generated.

The Intraparticle Diffusion Model. The possibility of using the intraparticle diffusion model as the sole mechanism was investigated according to the Weber-Moris equation (14):

$$q_e = C + kln\, t^{1/2} \quad (14)$$

where the constant kint (mg/min.) is the intraparticle diffusion constant ratio, and C is the boundary layer thickness [20].

If the rate limiting is only due to intra-particle diffusion, then qt vs $t^{1/2}$ gave a linear plot which passes through the origin. Otherwise, some other mechanism or factors, along with the intraparticle diffusion mechanism, may be responsible. From Table 3, it's clear that the intraparticle diffusion model is not applicable for the adsorption of MV onto CWL adsorbents since q_t vs $t^{1/2}$ does not pass through the origin. It can be concluded that intraparticle diffusion may not be the sole rate-determining step of the adsorption mechanism.

Table 3 – Calculated isotherm parameters for adsorption of Methyl violet onto RWL adsorbent

Isotherms	Parameters	Values
Langmuir	q_0 (mg/g)	98.04
	K_L (l/mg)	0.147
	R_L	0.056
	R^2	0.8151
Freundlich	1/n	1.4821
	N	0.6747
	K_F	18.247
	R^2	0.8024
Temkin	A_T	0.6456
	b_T	13.367
	B	185.350
	R^2	0.9225
D-R	q_s (mg/g)	383.907
	β (mol^2/kj^2)	$2.0x10^{-6}$
	ϵ (kJ/mol)	0.297
	R^2	0.9620

Isotherms Studies

The equilibrium data were generated and analysed based on four fundamental isotherms models: the Langmuir, Freunlich, Temkin and D-R. These models were used to explain or describe the adsorbents-adsorbates behavioural interaction and also understand the mechanism of the adsorption reaction rate pathways.

Langmuir Isotherm. According to this model, the adsorption of analytes takes place on the homogenous sites of the surface of the adsorbent with monolayer formation coverage [47], and can be expressed as:

$$q_e = \frac{q_0 K_l C_e}{1+K_l q_0} \quad (15)$$

The rearrangement of (15) gives:

$$\frac{1}{q_e} = \frac{1}{q_0} + \frac{1}{q_0 K_L C_e} \quad (16)$$

where q_e is the amount of MV retained at equilibrium by CWL adsorbent in mg/g, q_o is the monolayer adsorption capacity (mg/g), K_L is the Langmuir constant (l/mg), and C_e is the equilibrium concentration (mg/l) respectively. The K_L and q_o were determined from the slope and intercept of a graph of $1/q_e$ against $1/C_e$, respectively.

The dimensionless separation factor R_L is defined by relation as expressed in (17).

$$R_L = \frac{1}{1+K_L C_o} \quad (17)$$

where C_o is the maximum initial concentration (mg/g).

The R_L (separation factor) indicates whether the adsorption process is either unfavourable (R_L>1), linear (R_L=1), favourable (0<R_L<1), or irreversible (R_L = 0).

Freundlich Isotherm. This model described the adsorption process as irreversible and non-ideal, resulting in multi-layer coverage on the heterogeneous surface of the adsorbents [48]. This model can be expressed using (18).

$$q_e = K_f C_e \frac{1}{n} \quad (18)$$

The logarithm of both sides of (4) was taken to obtain the linear form as given in (19):

$$log q_e = log K_f + \frac{1}{n} log C_e \quad (19)$$

A plot of log(q_e) vs log(C_e) gives a straight line with slope and intercept to be 1/n and log(K_f), respectively.

Where qe is the number of adsorbates adsorbed in mg/g, C_e is the equilibrium concentration of the adsorbates in mg/l, K_f is the Freundlich constant related to maximum adsorption capacity, n is the Fruendlich constant related to maximum adsorption capacity (dimensionless).

Temkin Model. This model considers the interaction between adsorbent materials and adsorbate molecules to be adsorbed, assuming that the free energy of the adsorption process is a function of the surface coverage [49]. This isotherm is expressed by (20).

$$q_e = \frac{RT}{b_T} \ln A_T + \frac{RT}{b} \ln C_e \quad (20)$$

where R is the molar gas constant ($Jmol^{-1}K^{-1}$), T is the temperature in kelvin, b is the variation of adsorption energy (J/mol), and b_T is the equilibrium binding constant (l/mg) corresponding to the maximum binding power.

The values of β and A_T were obtained and tabulated in Table 3 from the slope and intercept of q_e against the ln(C_e) plot, respectively.

Dubinin-Rudushkevich Isotherm. This model is used to determine the adsorption behaviour of adsorbents towards the adsorbate using (21):

$$\ln q_e = \log q_0 - K \in^2 \quad (21)$$

where q_o represents the constant of D-R (mol/g), and K is the mean free energy of adsorption (kJ/mol) [50].

However, ϵ can be calculated using (22):

$$\epsilon = RTln(1 + \frac{1}{C_e}) \quad (22)$$

where C_e is the adsorbate equilibrium concentration, R is the ideal Gas constant (8.314 J/mol.K), and T is the temperature in Kelvin. The values of qo and K were obtained using slope and intercept from the plot of $\ln C_e$ against ϵ^2, respectively.

Table 3 shows the Langmuir, Freundlich, Temkin, and D-R isotherm constants for the adsorption of MV onto CWL adsorbents. The R^2 values computed suggested that the D-R isotherm model best conforms with the experimental data for the MV-CWL adsorption process. The equilibrium binding constant b_T and the heat of adsorption (ϵ) values were found to be 13.37 l/mg and 297.00 J/mol, respectively. As a result, physical adsorption is assumed for the interaction of CWL and MV.

Thermodynamic Studies

To describe the thermodynamic behaviour of the process of adsorption of dye pollutants from aqueous solution using carbonised water lily (CWL) leaves from thermodynamic parameters such as change of enthalpy (ΔH), entropy (ΔS) and Gibb's free energy (ΔG) was used (23)–(25).

$$K_c = \frac{C_s}{C_e} \quad (23)$$

The K_c for the adsorption of MV onto CWL adsorbents used in the study at different temperatures were calculated using (23). Gibb's free energy change (ΔG) was computed using the relation:

$$\Delta G = -RTlnK_c \quad (24)$$

However, other thermodynamics functions such as adsorption enthalpy (ΔH) & entropy change (ΔS) were obtained from the relation:

$$lnK_c = -\frac{\Delta H}{RT} + \frac{\Delta S}{R} \quad (25)$$

The ΔH and ΔS functions were determined from the slope and the intersection point of $\ln K_c$ versus the 1/T plot (Figure 6). Whereas Cs is the amount of adsorbate in the adsorbed phase and Ce signifies the remaining un-adsorbed MV concentration (mg/l) in the liquid phase at equilibrium time, T and R are temperature K and molar gas constant (8.314 $Jmol^{-1}k^{-1}$).

The values of the thermodynamic parameters obtained are reported in Table 4.

Table 4 – Thermodynamics parameters for adsorption of MV onto CWL adsorbent

T(K)	ln Kc	ΔG (kJ/mol)	ΔH (J/mol)	ΔS (J/mol.K)
303	4.041	-10.180	-3.01	23.77
313	4.023	-10.469		
323	3.989	-10.713		
333	3.932	-10.886		

Generally, the negative value of ΔG expresses the spontaneity and feasibility of MV adsorption onto CWL adsorbent. However, the magnitude of ΔG increase with increasing temperature, indicating the adsorption of MV-CWL to be conducive at higher temperatures [11]. The negative values of ΔH (-3.01 J/mol) manifest that the adsorption of MV onto CWL is an exothermic process and corresponds to the physio-sorption process (ΔH<10 kJ/mole). In contrast, the positive value of ΔS implies that the randomness at the solid/liquid interface during the adsorption process increases MV concentration at the solid/liquid interface [51].

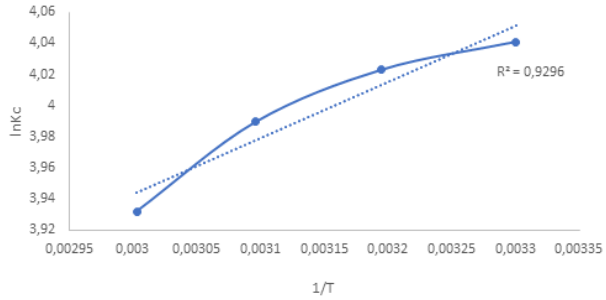

Figure 6 – Van't Hoff Plot for adsorption of MV-CWL

CONCLUSIONS

In this work, the suitability of carbonised water lily leaf-derived adsorbent for the adsorption of

methyl violet from an aqueous solution was evaluated in a series of batch adsorption experiments. The adsorbent surface was characterised using FTIR and SEM before and after adsorption to confirm the functional groups and morphology of the adsorbent's character responsible for the adsorption process. The adsorption of the methyl violet dye was affected by changes in contact time, adsorbent dosage, concentration, and pH. Kinetically, the MV adsorption onto CWL was found to follow the pseudo-second-order kinetic model, while the D-R adsorption isotherm model best describes the mechanism process. Thermodynamic studies confirmed that the process was spontaneous and exothermic, decreasing randomness on the system level during the adsorbent-liquid interface interaction.

Funding

This research received funding and assistance from Abubakar Tatari Ali Polytechnic, Bauchi, through Education Trust Fund (TETfund) Institution Based Research for the 2022 annual intervention.

Acknowledgements

The authors are grateful to Bayero University Central Laboratory and Abubakar Tatari Ali Polytechnic, Bauchi in Nigeria, for providing facilities for this study.

Conflict of Interest

The authors declare no conflict of interest.

REFERENCES

1. Muhd Din, A. T., & Hameed, B. H (2010). Adsorption of methyl violet on acid modified activated carbons: Isotherms and Thermodynamics. *Journal of Applied Science in environmental Sanitation, 5*(N), 151–160.

2. Safarzadeh, H., Peighambardoust, S. J., Mousavi, S. H., Mohammadi, R., & Peighambardoust, S. H. (2022). Adsorption of methyl violet dye from wastewater using poly(methacrylic acid-co-acrylamide)/bentonite nanocomposite hydrogels. *Journal of Polymer Research, 29*(4). doi: 10.1007/s10965-022-02956-0

3. Nhung, N. T. H., Quynh, B. T. P., Thao, P. T. T., Bich, H. N., & Giang, B. L. (2018). Pretreated Fruit Peels as Adsorbents for Removal of Dyes from Water. *IOP Conference Series: Earth and Environmental Science, 159*, 012015. doi: 10.1088/1755-1315/159/1/012015

4. Ajji, Z., & Ali, A. M. (2007). Adsorption of methyl violet and brilliant blue onto poly(vinyl alcohol) membranes grafted with N-vinyl imidazole/acrylic acid. *Nuclear Instruments and Methods in Physics Research Section B: Beam Interactions with Materials and Atoms, 265*(1), 362–365. doi: 10.1016/j.nimb.2007.09.004

5. Raghu, S., & Ahmed Basha, C. (2007). Chemical or electrochemical techniques, followed by ion exchange, for recycle of textile dye wastewater. *Journal of Hazardous Materials, 149*(2), 324–330. doi: 10.1016/j.jhazmat.2007.03.087

6. Chen, F., Liu, X., Yu, C., Chen, Y., Tang, H., & Zhang, L. (2017). Water lilies as emerging models for Darwin's abominable mystery. *Horticulture Research, 4*(1). doi: 10.1038/hortres.2017.51

7. Tani, M., Sawada, A., & Oyabu, T (2006). Ability of water lilies to purify water polluted by soap and their applications in domestic sewage disposal facilities. *Sensors and materials, 18*(2), 91–101.

8. Phatai, P., Utara, S., & Hatthapanit, N. (2013). Removal of Methyl Violet by Adsorption onto Activated Carbon Derived from Coffee Residues. *Advanced Materials Research*, 864–867, 710–714. doi: 10.4028/www.scientific.net/amr.864-867.710

9. Bonetto, L. R., Ferrarini, F., de Marco, C., Crespo, J. S., Guégan, R., & Giovanela, M. (2015). Removal of methyl violet 2B dye from aqueous solution using a magnetic composite as an adsorbent. *Journal of Water Process Engineering, 6*, 11–20. doi: 10.1016/j.jwpe.2015.02.006

10. Saravanan, N., & Rathika, G. (2018). Adsorption Studies of Methyl Violet Dye using Biosorbents. *International Journal of ChemTech Research, 11*(7), 84–94. doi: 10.20902/ijctr.2018.110711

11. Zhai, H., Zou, J., Liu, F., Chen, F., Yan, X., & Zhou, W. (2020). Adsorption removal of methyl violet from aqueous solution by chromium phosphovanadate. *Surface and Interface Analysis, 53*(1), 76–83. doi: 10.1002/sia.6874

12. You, X., Zhou, R., Zhu, Y., Bu, D., & Cheng, D. (2022). Adsorption of dyes methyl violet and malachite green from aqueous solution on multi-step modified rice husk powder in single and binary systems: Characterisation, adsorption behavior and physical interpretations. *Journal of Hazardous Materials, 430*, 128445. doi: 10.1016/j.jhazmat.2022.128445

13. Foroutan, R., Mohammadi, R., Ahmadi, A., Bikhabar, G., Babaei, F., & Ramavandi, B. (2022). Impact of ZnO and Fe3O4 magnetic nanoscale on the methyl violet 2B removal efficiency of the activated carbon oak wood. *Chemosphere, 286*, 131632. doi: 10.1016/j.chemosphere.2021.131632

14. Geremew, B., & Zewde, D. (2022). Hagenia abyssinica leaf powder as a novel low-cost adsorbent for removal of methyl violet from aqueous solution: Optimisation, isotherms, kinetics, and thermodynamic studies. *Environmental Technology & Innovation, 28*, 102577. doi: 10.1016/j.eti.2022.102577

15. Syakina, A. N., & Rahmayanti, M. (2023). Removal of Methyl Violet from Aqueous Solutions by Green Synthesized Magnetite Nanoparticles with Parkia Speciosa Hassk. *Peel Extracts*. doi: 10.2139/ssrn.4329442

16. Gaya, U. I., Otene, E., & Abdullah, A. H. (2015). Adsorption of aqueous Cd(II) and Pb(II) on activated carbon nanopores prepared by chemical activation of doum palm shell. *SpringerPlus, 4*(1). doi: 10.1186/s40064-015-1256-4

17. Anisuzzaman, S. M., Joseph, C. G., Daud, W. M. A. B. W., Krishnaiah, D., & Yee, H. S. (2014). Preparation and characterisation of activated carbon from Typha orientalis leaves. *International Journal of Industrial Chemistry, 6*(1), 9–21. doi: 10.1007/s40090-014-0027-3

18. Ibrahim, M. B., & Sani, S. (2015). Neem (Azadirachta indica) Leaves for Removal of Organic Pollutants. *Journal of Geoscience and Environment Protection, 3*(2), 1–9. doi: 10.4236/gep.2015.32001

19. Amode, J. O., Santos, J. H., Md. Alam, Z., Mirza, A. H., & Mei, C. C. (2016). Adsorption of methylene blue from aqueous solution using untreated and treated (Metroxylon spp.) waste adsorbent: equilibrium and kinetics studies. *International Journal of Industrial Chemistry, 7*(3), 333–345. doi: 10.1007/s40090-016-0085-9

20. Muhammad, A. A., & Aondofa, N. T. (2020). Paraquat dichloride adsorption from aqueous solution using Carbonized Bambara Groundnut Vigna subterranean) Shells. *Bayero Journal of Pure and Applied Sciences, 12*(1), 167–177. doi: 10.4314/bajopas.v12i1.28s

21. Giwa, S. O., Moses, J. S., Adeyi, A. A., & Giwa, A. (2018). Adsorption of Atrazzine from aqueous solution using Desert Date Seed Shell activated carbon. *ABUAD Journal of Engineering Research & Development, 1*(3), 317–325.

22. Muhd Din, A.T., Yew, H. F. C., & Malik, A (2009). A liquid-phase batch adsorption study of methyl violet dye removal using acid modified activated carbon. *16th ASEAN Regional Symposium on Chemical Engineering*. Retrieved from https://www.researchgate.net/publication/271967433_A_Liquid-Phase_Batch_Adsorption_Study_of_Methyl_Violet_Dye_Removal_Using_Acid_Modified_Activated_Carbon

23. Manjunatha, K. R., & Vagish, M (2016). Study on adsorption efficacy of neem leaves powder in the removal of reactive red dye colour from aqueous solution. *International Research Journal Engineering & Technology, 3*, 12–24.

24. Majithiya, D., Yadav, A., & Tawde, S. (2013). Comparative studies of Azidirachta indica (Neem) leaf powder and activated carbon as an adsorbent for removal of chromium from an aqueous solution. *Journal of environmental science and sustainability, 1*(1), 21–27.

25. Dülger, Ö., Turak, F., Turhan, K., & Özgür, M. (2013). Sumac Leaves as a Novel Low-Cost Adsorbent for Removal of Basic Dye from Aqueous Solution. *ISRN Analytical Chemistry, 2013*, 1–9. doi: 10.1155/2013/210470

26. Shahryari, Z., Goharrizi, S.A., & Azadi, M. (2010). Experimental study of methylene blue adsorption from aqueous solutions onto carbon nano tube. *International Journal of water Resources and environmental engineering, 2*(2), 016–028.

27. Sartape, A. S., Mandhare, A. M., Jadhav, V. V., Raut, P. D., Anuse, M. A., & Kolekar, S. S. (2017). Removal of malachite green dye from aqueous solution with adsorption technique using Limonia acidissima (wood apple) shell as low cost adsorbent. *Arabian Journal of Chemistry, 10*, S3229–S3238. doi: 10.1016/j.arabjc.2013.12.019

28. Xiong, W., Tong, J., Yang, Z., Zeng, G., Zhou, Y., Wang, D., Song, P., Xu, R., Zhang, C., & Cheng, M. (2017). Adsorption of phosphate from aqueous solution using iron-zirconium modified activated carbon nanofiber: Performance and mechanism. *Journal of Colloid and Interface Science, 493*, 17–23. doi: 10.1016/j.jcis.2017.01.024

29. Jimoh, A. O., Namadi, M. M., Ado, K., & Muktar, B. (2016). Proximate and Ultimate Analysis of Eichornia natans (Water Hyacinth), Pistia stratiotes (Water Lettuce) and Nymphaea lotus (Water Lily) in the Production of Biofuel. *Advances in Applied Research, 7*(4), 243–249.

30. Efomah, A. N., & Gbabo, A. (2015). The Physical, Proximate and Ultimate Analysis of Rice Husk Briquettes Produced from a Vibratory Block Mould Briquetting Machine. *International Journal of Innovative Science, Engineering and Technology, 2*(5), 814–822.

31. Bello, O. S., Adegoke, K. A., & Akinyunni, O. O. (2015). Preparation and characterisation of a novel adsorbent from Moringa oleifera leaf. *Applied Water Science, 7*(3), 1295–1305. doi: 10.1007/s13201-015-0345-4

32. Okieimen, F. E., Okieimen, C. O., Wuana, R. A. (2007). Preparation and characterisation of activated carbon from rice husk. *Journal of Chemical Society, 32*(1), 126–136.

33, Bekçi, Z., Seki, Y., & Cavas, L. (2009). Removal of malachite green by using an invasive marine alga Caulerpa racemosa var. cylindracea. *Journal of Hazardous Materials, 161*(2–3), 1454–1460. doi: 10.1016/j.jhazmat.2008.04.125

34. Pradeep Sekhar, C., Kalidhasan, S., Rajesh, V., & Rajesh, N. (2009). Bio-polymer adsorbent for the removal of malachite green from aqueous solution. *Chemosphere, 77*(6), 842–847. doi: 10.1016/j.chemosphere.2009.07.068

35, Bello, O. S., & Ahmad, M. A. (2011). Response Surface Modeling and Optimisation of Remazol Brilliant Blue Reactive Dye Removal Using Periwinkle Shell-Based Activated Carbon. *Separation Science and Technology, 46*(15), 2367–2379. doi: 10.1080/01496395.2011.595756

36. Bello, O. S., & Ahmad, M. A (2011). Adsorption of dyes from aqueous solution using chemical activated mango peels. *2nd International Conference on Environmental Science and Technology, 2*, 108–113.

37. Vimonses, V., Lei, S., Jin, B., Chow, C. W. K., & Saint, C. (2009). Kinetic study and equilibrium isotherm analysis of Congo Red adsorption by clay materials. *Chemical Engineering Journal, 148*(2–3), 354–364. doi: 10.1016/j.cej.2008.09.009

38. Abubakar, A., & Batagarawa, S. M. (2018). Kinetic and isotherm studies of malachite green and Congo red adsorption from aqueous solution by corn stalk bio-waste material. *Bayero Journal of Pure and Applied Sciences, 10*(1), 350. doi: 10.4314/bajopas.v10i1.70s

39. Li, K., Zheng, Z., Huang, X., Zhao, G., Feng, J., & Zhang, J. (2009). Equilibrium, kinetic and thermodynamic studies on the adsorption of 2-nitroaniline onto activated carbon prepared from cotton stalk fibre. *Journal of Hazardous Materials, 166*(1), 213–220. doi: 10.1016/j.jhazmat.2008.11.007

40. Özacar, M., & Şengil, İ. A. (2005). Adsorption of metal complex dyes from aqueous solutions by pine sawdust. *Bioresource Technology, 96*(7), 791–795. doi: 10.1016/j.biortech.2004.07.011

41. Abdus-Salam, N., & Adekola, S. K. (2018). Adsorption studies of zinc(II) on magnetite, baobab (Adansonia digitata) and magnetite–baobab composite. *Applied Water Science, 8*(8). doi: 10.1007/s13201-018-0867-7

42. Dahri, M. K., Kooh, M. R. R., & Lim, L. B. L. (2013). Removal of Methyl Violet 2B from Aqueous Solution UsingCasuarina equisetifoliaNeedle. *ISRN Environmental Chemistry, 2013*, 1–8. doi: 10.1155/2013/619819

43. Li, C., Zhang, X., Pan, J., Xu, P., Liu, Y., Yan, Y., & Zhang, Z. (2009). Strontium(II) Ion Surface-Imprinted Polymers Supported by Potassium Tetratitanate Whiskers: Synthesis, Characterisation and Adsorption Behaviours. *Adsorption Science & Technology, 27*(9), 845–859. doi: 10.1260/0263-6174.27.9.845

44. Gautam, R. K., Mudhoo, A., Lofrano, G., & Chattopadhyaya, M. C. (2014). Biomass-derived biosorbents for metal ions sequestration: Adsorbent modification and activation methods and adsorbent regeneration. *Journal of Environmental Chemical Engineering, 2*(1), 239–259. doi: 10.1016/j.jece.2013.12.019

45. Pan, X., & Zhang, D (2009). Removal of malachite green from water by firmiana simplex wood fiber. *E-journal of Biotechnology, 12*(4). Retrieved from https://www.scielo.cl/scielo.php?script=sci_arttext&pid=S0717-34582009000400009

46. Ayuba, A. M., & Abdulmumini, H. (2022). Raw water lily leaves (Nymphaea Lotus) powder as an effective adsorbent for adsorption of malachite green dye from aqueous solution. *Chemical Review and Letters, 5*, 250–260.

47. Ullah, S., Ur Rahman, A., Ullah, F., Rashid, A., Arshad, T., Viglašová, E., Galamboš, M., Mahmoodi, N. M., & Ullah, H. (2021). Adsorption of Malachite Green Dye onto Mesoporous Natural Inorganic Clays: Their Equilibrium Isotherm and Kinetics Studies. *Water, 13*(7), 965. doi: 10.3390/w13070965

48. Dehghani, M. H., Farhang, M., Alimohammadi, M., Afsharnia, M., & Mckay, G. (2018). Adsorptive removal of fluoride from water by activated carbon derived from CaCl2-modified Crocus sativus leaves: Equilibrium adsorption isotherms, optimisation, and influence of anions. *Chemical Engineering Communications, 205*(7), 955–965. doi: 10.1080/00986445.2018.1423969

49. Aondofa, N. T., Ayuba, A. M. (2020). Kinetic and equilibrium studies of paraquat dichloride adsorption of raw Bambara groundnut (Vigna subterranean) shells. *Applied Journal of Environmental Engineering Sciences, 6*(1), 1–13.

50. Nica, C., Zaharia, R.I., Boron, S., & Coseri, D. S. (2020). Adsorptive materials based on preparation, characterisation and application of copper iron retention. *Cellulose Chemistry Technology, 54*(5-6), 579–590.

51. Belala, Z., Jeguirim, M., Belhachemi, M., Addoun, F., & Trouvé, G. (2011). Biosorption of basic dye from aqueous solutions by Date Stones and Palm-Trees Waste: Kinetic, equilibrium and thermodynamic studies. *Desalination, 271*(1–3), 80–87. doi: 10.1016/j.desal.2010.12.009